

Particle capture into the lung made simple?

Talita Felipe de Vasconcelos,^{1,2} Bernard Sapoval,^{1,3} José S. Andrade, Jr.,² James B. Grotberg,⁴ Yingying Hu,⁴ and Marcel Filoche^{1,3,*}

¹Physique de la Matière Condensée, Ecole Polytechnique, CNRS, Palaiseau, France; ²Departamento de Física, Universidade Federal do Ceará, Ceará, Brazil; ³CMLA, ENS Cachan, CNRS, UniverSud, Cachan, France; and ⁴Department of Biomedical Engineering, University of Michigan, Ann Arbor, Michigan

Submitted 4 August 2010; accepted in final form 9 March 2011

de Vasconcelos TF, Sapoval B, Andrade JS Jr, Grotberg JB, Hu Y, Filoche M. Particle capture into the lung made simple? *J Appl Physiol* 110: 1664–1673, 2011. First published March 17, 2011; doi:10.1152/jappphysiol.00866.2010.—Understanding the impact distribution of particles entering the human respiratory system is of primary importance as it concerns not only atmospheric pollutants or dusts of various kinds but also the efficiency of aerosol therapy and drug delivery. To model this process, current approaches consist of increasingly complex computations of the aerodynamics and particle capture phenomena, performed in geometries trying to mimic lungs in a more and more realistic manner for as many airway generations as possible. Their capture results from the complex interplay between the details of the aerodynamic streamlines and the particle drag mechanics in the resulting flow. In contrast, the present work proposes a major simplification valid for most airway generations at quiet breathing. Within this context, focusing on particle escape rather than capture reveals a simpler structure in the entire process. When gravity can be neglected, we show by computing the escape rates in various model geometries that, although still complicated, the escape process can be depicted as a multiplicative escape cascade in which each elementary step is associated with a single bifurcation. As a net result, understanding of the particle capture may not require computing particle deposition in the entire lung structure but can be abbreviated in some regions using our simpler approach of successive computations in single realistic bifurcations. Introducing gravity back into our model, we show that this multiplicative model can still be successfully applied on up to nine generations, depending on particle type and breathing conditions.

pulmonary airways; particle deposition; aerodynamics; multiplicative cascade

THE DEPOSITION PROCESS into an aerodynamic tree is complex because it results from the interplay between the fluid velocity map in the branched structure, which depends on fluid density and viscosity (1, 4, 5, 17, 25, 30, 34), and the distribution of particle sizes, masses, and velocities (13, 14, 35). Over the past 20 yr, many reports have been devoted to the analysis of this process. These studies explore increasingly complex structures: two- or three-dimensional structures with an increasing number of generations (6, 16), detailed branching morphologies (2, 3, 21, 23, 24, 28, 31), and a wide range of aerosol types and aerodynamic effects (15, 20).

One of the difficulties in understanding the particle capture in such systems comes from the fact that each particle follows a complicated trajectory, with each part of this trajectory depending on the detailed structure of the flow (1, 30). Even at small enough Reynolds numbers (Re), although deterministic, the detailed complexity of each trajectory suggests that a global approach would be

even more out of reach. But, as shown in this report, this is not true. A global statistical description, at the level of a population of particles, permits us to derive simple laws for the escape rate (E) and capture rates (C) averaged among the entire population of incoming particles. E represents the fraction of incoming particles that cross a given structure without being captured, and C is the fraction of particles captured in this structure (also called deposition efficiency), so that $E + C = 1$. It will be clear in the following that what is simple in the trapping in an aerodynamic tree is not the capture but the escape, which essentially multiplies in successive bifurcations, a fact that has been so far obscured by the complexity of global tree studies.

METHODS

The physical model. For each structure, we solved the steady-state Navier-Stokes and continuity equations corresponding to an inspiration flow (from the entrance to the outlets) for various Re , as follows:

$$\rho(\vec{u} \cdot \vec{\nabla})\vec{u} = -\vec{\nabla}p + \mu\nabla^2\vec{u} \quad (1)$$

with

$$\vec{\nabla} \cdot \vec{u} = 0 \quad (2)$$

where ρ is the fluid (air)-specific mass, $\vec{\nabla}$ is the gradient operator, \vec{u} is the fluid velocity, μ is the fluid viscosity, and p is the pressure. Using the diameter of the first branch (D_0) and the mean entrance velocity of the fluid (u_0) as units, the entrance Re is defined as follows: $Re = \rho u_0 D_0 / \mu = u_0 D_0 / \nu$, where ν is the kinematic viscosity of air (0.15 cm²/s). The Re is the only dimensionless parameter governing Eqs. 1 and 2.

Nonslip boundary conditions were imposed on the lateral walls of the branching tree. Additional dimensionless parameters entered here through the geometry discussed below. The velocity field was taken as uniform at the entrance cross section and constant pressure conditions were assumed on the outlets of the structure.

After each flow simulation, the particle trajectories and deposition were computed by numerically solving Newton's second law for each particle with a Stokes drag force (\vec{F}_{drag}) written for a spherical particle as follows: $\vec{F}_{\text{drag}} = 3\pi\mu d_p(\vec{u} - \vec{u}_p)$, where d_p is the particle diameter and \vec{u}_p is the particle velocity. This is a simplified expression of the drag force when the so-called "particle Re " (Re_p ; defined as $Re_p = u_p D / \nu$) remains small, a good approximation here. The resulting equation of motion of a particle of mass m can be written as follows:

$$m \frac{d\vec{u}_p}{dt} = (3\pi\mu d_p)(\vec{u} - \vec{u}_p) \quad (3)$$

The quantity $m(3\pi\mu d_p)$ is the relaxation time τ , which measures the time for the particle to adjust to the flow (1). The Stokes number (St), often called the impaction parameter, is the ratio of the relaxation time to a characteristic transit time for the flow D/u_0 . For spherical particles,

Address for reprint requests and other correspondence: M. Filoche, Physique de la Matière Condensée, Ecole Polytechnique, Palaiseau 91128, France (e-mail: marcel.filoche@polytechnique.edu).

$$St = \frac{\tau}{(D/u_0)} = \frac{\rho_p d_p^2 u_0}{18\mu D}$$

In the expression of St , ρ_p is the particle-specific mass and D is the diameter of the branch. The St is the second dimensionless parameter governing Eq. 3 for a given airway geometry.

Diffusion and gravity effects are not taken into account in this approach for the moment, as the goal is here to derive the general background properties of the deposition process in a tree structure. Thus, the inertia of the particle and the drag force exerted by the fluid are the only two ingredients that cannot be removed. We will discuss later the relative importance of gravity and diffusion and how they can be introduced as well as other physical effects. Without approximation, this study is about the deposition of particles transported by convection in a tree in the absence of gravity or in a microgravity environment (7–10). The particles were assumed to be large enough so that diffusion can be ignored.

Geometry of the tree. The tracheobronchial tree is a complex branching structure that exhibits self-similar invariance at all scales. A cast of the airways showing this complexity is shown in Fig. 1A. The geometrical airway models are dichotomous branching trees (see Fig. 1, B and C). All branches have the same aspect ratio, namely, their length-to-diameter ratio (L/D) = 3, a commonly admitted value for the intermediate bronchial tree in mammalian lungs, where we focused our attention. Each branching is a symmetric coplanar bifurcation described by the branching angle (θ) between the daughter branches and the diameter ratio (h) = D_{i+1}/D_i of successive generations, where i is the generation number. Also, the azimuthal angle (α) between successive bifurcation planes was specified.

We defined the canonical tree by the following parameters: $h = 2^{-1/3}$, $\theta = 60^\circ$, and $\alpha = 90^\circ$. It has to be noted that this tree corresponds to Weibel's "A" symmetric model (33).

Method of solution. For fixed geometrical parameters, the flow distribution (\vec{u}) was first computed for each tree structure using a parallel commercial CFD code (Fluent) on a computer Linux cluster to solve Eqs. 1 and 2. For each flow (each Re value) simulation, 10,000 particles, uniformly distributed in the entrance cross section, were launched with an initial velocity equal to the local fluid velocity, and their trajectories were calculated by the numerical integration of Eq. 3. When a particle trajectory crossed the surface at a given point, the particle was considered to be trapped there, and the number of particles captured in each branch was calculated.

We then obtained a map of the particle deposition along the tree. C was defined as the number of particles that impacted at the inner surface divided by the number of particles at the entrance. E was simply calculated as $E = 1 - C$.

RESULTS

We first computed the capture efficiency in the canonical tree ($h = 2^{-1/3}$, $\theta = 60^\circ$, $\alpha = 90^\circ$) of four generations (3 bifurcation levels and 8 outlets; see Fig. 1B) for different values of Re (50, 100, 500, 1,300, and 2,600). C is plotted in Fig. 2A in the traditional way in which investigators have presented their results. Figure 2B, on the other hand, shows the corresponding plot of E . As shown in Fig. 2, A and B, all data almost collapsed onto the same curve through the entire range of St . The capture process in the tree thus appears to depend essentially on the St of the population of particles entering the tree, a commonly known fact in deposition studies (18, 29, 35).

Figure 3 shows, with $Re = 50$, the total escape rate for the entire tree (E_t), the escape rate for the first bifurcation (E_1), and the escape rate for the second bifurcation (E_2) [with E_n defined as the number of particles that escaped bifurcation (n) divided by the number of particles that entered it]. E_1 and E_2 were almost identical: although the population arriving on the second bifurcation could be thought to have different spatial and velocity distributions than the population arriving on the first bifurcation, both appeared to have the same E value.

The most striking result of this work arises from the comparison of particle capture in the entire tree with particle capture computed independently in single bifurcations. Specifically, E in the whole four-generation tree was compared with the product of the E values computed separately for the three successive single bifurcations. The result is shown in Fig. 4, A and B, which results in a simple, and therefore interesting, answer: when plotted against the St of incoming particles, the average E value of a four-generation tree remarkably fits the product of E values for three successive bifurcation levels, computed independently (Fig. 4A). All bifurcations can be thus considered as identical units of particle capture, i.e., with the same escape probability. This multiplicative behavior of E was carried out for the same parameter values shown in Fig. 4A for one seven-generation tree with six levels of bifurcations. The same result was obtained and is shown in Fig. 4B: the E value of the seven-generation tree can be considered as the product of the E values of six individual and identical E values.

In other words, from a statistical point of view, the capture process in a tree for a large population of particles can be seen

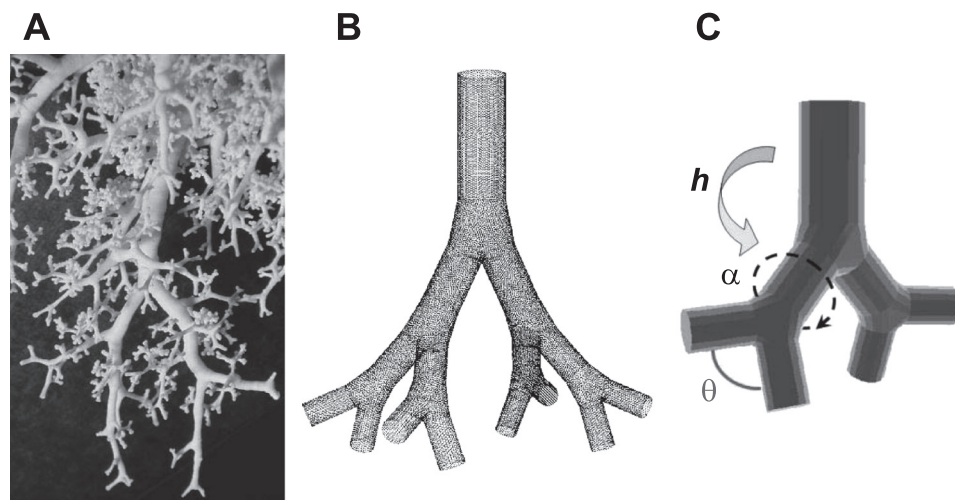


Fig. 1. A: cast of the human intermediate bronchial tree (courtesy of E. R. Weibel). B: geometrical model used for the numerical simulations (4 generations; hence, 3 successive bifurcations). C: the geometrical parameters of the model geometry are the diameter ratio (h) between successive generations, the branching angle (θ), and the azimuthal angle (α) between successive bifurcation planes.

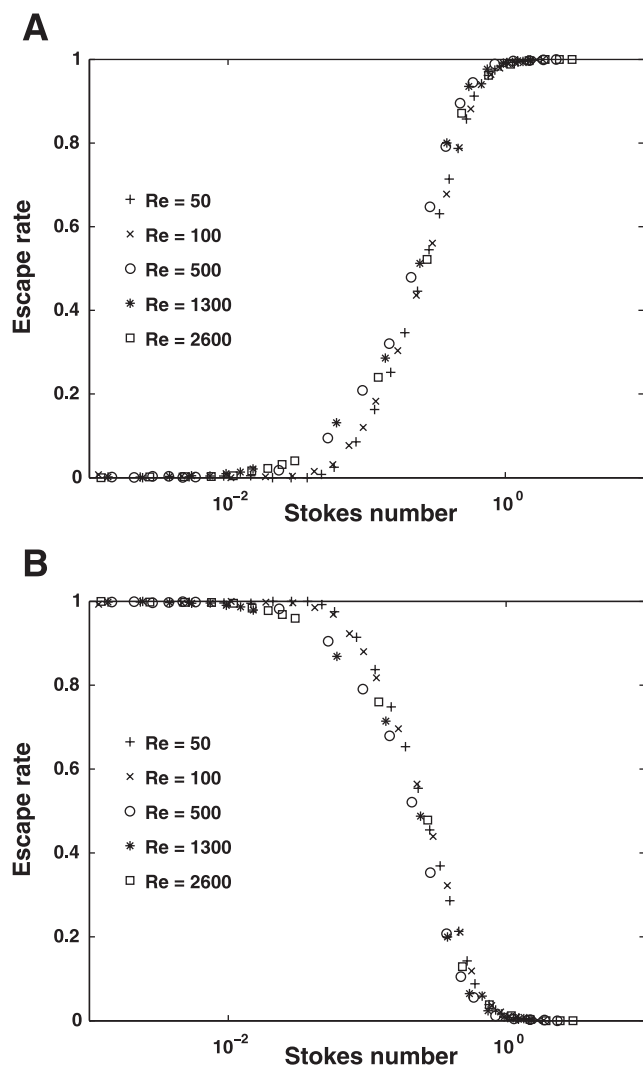


Fig. 2. A: capture rate versus $\log_{10}(St)$, where St is the Stokes number, in a four-generation tree for five values of the Reynolds number (Re). B: escape rate versus $\log_{10}(St)$ in the same tree for five values of the Re .

as a succession of independent trials at each bifurcation as the population progresses in the more distal regions. This suggests that, in the goal to understand only deposition, the geometry of the bronchial tree should not be considered as an assembly of successive branches (Fig. 5A) but as an assembly of successive bifurcations (Fig. 5B). Such a multiplicative property has already been used between different regions of the airway system (nasal, larynx, upper bronchial tree, etc.) to model deposition efficiency (13). The strong difference here is that we show this multiplicative property also holds for successive bifurcations within the airway tree. This allows us to propose a predictive probabilistic model from first principles, fundamentally different from an a posteriori statistical description (22).

Note that the multiplicative property mentioned above has been obtained for specific trees in which all bifurcations are reduced copies of one bifurcation (e.g., same θ and h) and for a constant α of 90° . We now see that this multiplicative property is robust in the sense that it holds for a very broad class of bifurcations and tree morphologies.

Particle escape properties of a single bifurcation. Very generally, the flow distribution in a bifurcation depends on the bifurcation geometry (represented by the parameters h and θ) and on the Re that governs fluid dynamics. The particle trajectories depend on the particle properties, mass (m_p) and possibly shape, through the drag force that characterizes the interaction between the particles and flow. But when studying C against one of these parameters, it seems difficult to summarize the capture process into a simple law. If, however, E across one single bifurcation is plotted against the St of the incoming particles, then all curves almost collapse onto a single curve for any values of Re (see Fig. 6). A slight departure from the universal collapse can be observed for a Re larger than a few hundreds. Indeed, for higher Re , the fluid streamlines have higher curvatures that the particles cannot follow. This consequently favors the capture by impaction in the bifurcation and lowers the escape. Also, at higher Re , the volume flow rate into the daughter tubes of a bifurcation may not be the same.

The capture (or escape) process in a single bifurcation was also observed to mostly depend on θ . To show that, we investigated the influence of the geometrical parameters θ and h on E of advected particles crossing the bifurcation. The results are shown in Fig. 7A and demonstrate that h has a very limited impact, whereas the results shown in Fig. 7B demonstrate that θ influences E only for particles of an initial St between 0.1 and 10.

In summary, E of a single bifurcation is a function of the St [$E(St)$] parameterized by θ and h and is almost independent of the Re . This function is the elementary building block that one can now use to understand the capture process as a statistical mechanism in the entire tree. In addition, note that, since E across an individual bifurcation only depends on one side on the St of the particles and on the other side on h and θ , there is no explicit dependency on the actual size of the bifurcation. It means that two individual bifurcations of different sizes but which are homothetic share the same escape function $E(St)$.

Particle escape properties of a tree as a cascade process. The multiplicative property exhibited in our first results (Fig. 4) suggests that each bifurcation captures particles indepen-

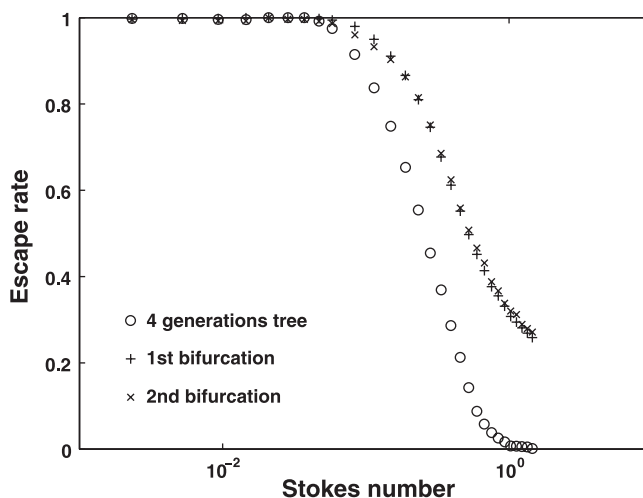


Fig. 3. Escape rates after the first and second bifurcation of a four-generation tree and global escape rate. One can see that the escape rates of the first and second bifurcation are identical.

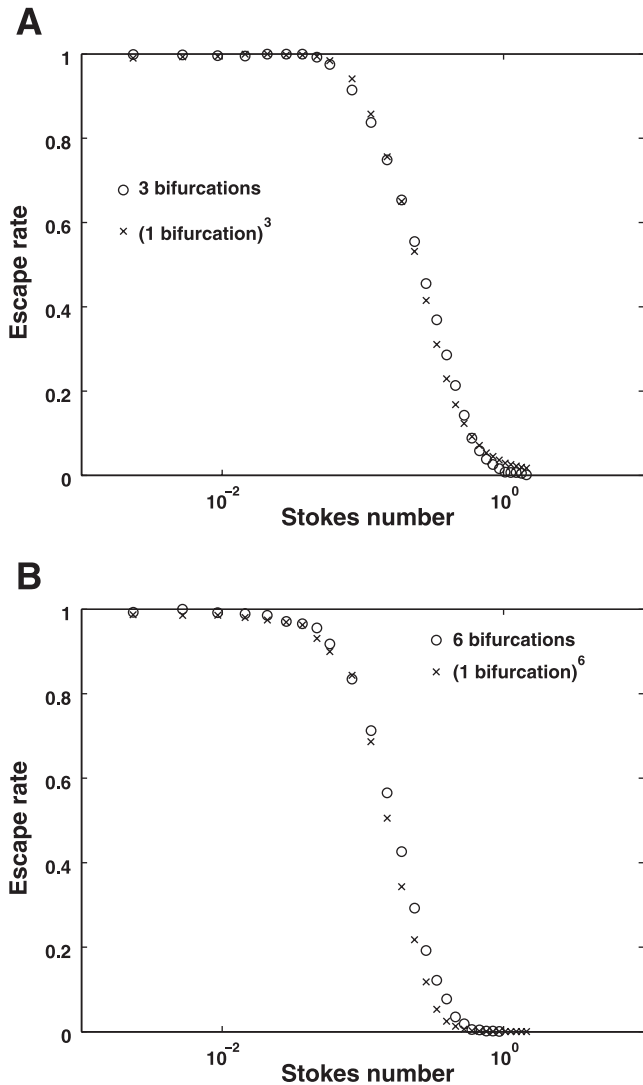


Fig. 4. A: statistical independence of the capture rates at each bifurcation level for a four-generation tree (3 successive bifurcation levels). The escape rate of the total structure, plotted against the St of the particles at the entrance, was almost equal to the escape rate of the entrance bifurcation multiplied by the escape rate of one successive elementary bifurcation raised to the square power. Although each particle may follow a complicated path, the global capture phenomenon statistically appears as purely multiplicative. B: the same result was obtained for a seven-generation tree.

dently of the others for low Re . Identifying E across each individual bifurcation as an escape probability, one can thus compute the global E across the entire tree by simply multiplying the E values along each possible path, with all paths being equally weighted since all bifurcations are symmetric.

One necessary condition for this multiplicative property to hold is that α , which is the geometrical parameter connecting one bifurcation to the next, plays a negligible role in the global E . To test this hypothesis, E was computed for various values of α between successive bifurcations. The result of these simulations is shown in Fig. 8. The almost nearly identical overlap of the curves, for any value of α , confirms that this parameter had very little influence on the global E in the tree. In other words, the capture process in the entire aerodynamic tree can be effectively computed by knowing only E across each elementary bifurcation.

Thus, the only remaining parameter needed to compute E of a population of particles entering a bifurcation is its characteristic St . A scaling relation of the St between two successive generations i and $i + 1$ can be deduced from a simple flux conservation equation. If u_i and D_i are the fluid velocity and branch diameter at generation i , respectively, then the flux conservation is as follows: $2\pi D_{i+1}^2 u_{i+1} = \pi D_i^2 u_i$, which means that the fluid velocity scales from one generation to the next as $(2h^2)^{-1}$ and that the St scales as $(2h^3)^{-1}$. Thus, the multiplicative property of E for a particle entering a three-bifurcation tree with an entrance St (St_E) is as follows:

$$E_i(St_E) = E_{h_1}(St_E) \times E_{h_2}\left(\frac{St_E}{2h_1^3}\right) \times E_{h_3}\left(\frac{St_E}{4h_1^3 h_2^3}\right) \quad (4)$$

where E_t is the E value of the whole tree; h_1 , h_2 , and h_3 are the h values for the first, second, and third bifurcations; and E_{h_1} , E_{h_2} , and E_{h_3} are the E values of each of these bifurcations. Once again, these elementary E values depend, if only weakly, on h and θ . Note that the h value of each bifurcation appears in two different ways in this equation: first, it influences, in a weak manner, the function $E(St)$ of the corresponding bifurcation, and, second, more importantly, it modifies the St of the particle before and after the bifurcation.

The result shown in Fig. 4 corresponds to a self-similar tree of constant h ($h_c = 2^{-1/3} \approx 0.79$). In this very specific case, the St remains constant along the tree and the multiplicative relation (4) simply becomes $E_3 = E_1^3$ or, expressed in terms of C , $C_3 = 1 - (1 - C_1)^3$.

To test the robustness of the multiplicative property when h values may vary in the tree, E was computed in a four-generation tree in which the h values of the first, second, and third generations were 0.79, 0.6, and 0.9, respectively. The global E was then compared with the product of E values for each generation, as expressed in Eq. 4. The good quantitative agreement between both curves shows that the multiplicative property also holds in this case (see Fig. 9).

A simple and universal model of capture, or escape, by impaction. This robustness of the multiplicative mechanism allows the formulation of a general analytic model for the trapping of particles into an aerodynamic tree of N generations. If one considers a tree in which the diameter ratio h_i is given for each generation, then E of particles entering this tree with St may escape with a rate determined by the following:

$$E_i(St) = \prod_{i=1}^N E_i(St_{i-1}) \quad \text{with} \quad St_0 = St \quad \text{and} \quad St_i = \frac{1}{2h_i^3} \times St_{i-1} \quad (5)$$

where E_i is the E value of the elementary bifurcations at each generation. E_i depends on the St of the particle, h , and θ , but not on α . E_i also does not depend on Re except for Re larger than a few hundreds, for which one has to apply a slight correction. In the case of a true self-similar tree, i.e., when h is identical for all generations, the global E is as follows:

$$E_i(St) = \prod_{i=1}^N E\left[\frac{St}{(2h^3)^i}\right] = E(St) \times E\left(\frac{St}{2h^3}\right) \times E\left(\frac{St}{4h^6}\right) \times \dots \times E\left[\frac{St}{(2h^3)^{N-1}}\right] \quad (6)$$

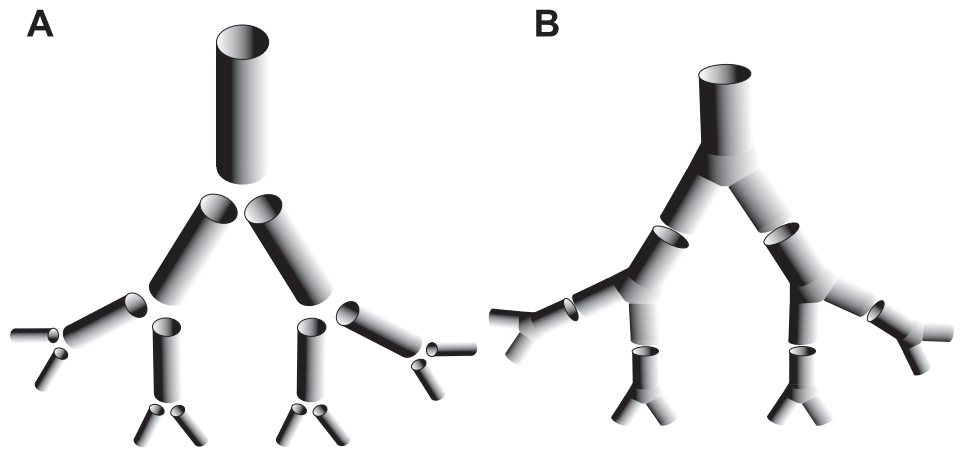


Fig. 5. The airway tree seen as a series of homothetic branches (A) or homothetic bifurcations (B).

with the elementary E being a “S”-shaped function that depends only on the geometry of the individual bifurcation.

In this model, all particles were assumed to be independent and without interaction, which means that for a population of two different particle types or sizes, the total C (resp. E) is simply computed by adding the C values (resp. E) of each separate type weighted by their proportion in the whole population. For a continuous distribution of particle sizes, the sum is replaced by an integral.

A critical geometrical threshold for trapping particles. An important consequence of this multiplicative behavior can be deduced by noticing that in a self-similar tree of constant h (h_c), the St of a particle evolves in a monotonous way when traveling deeper into the tree. The St will remain constant if h is equal to the critical value $h_c \approx 0.79$; it will increase if h is smaller and decrease if h is larger. Since the elementary capture rate is an S-shaped function of St going from 1 at low St to 0 at large St , it implies that, for a value of h larger than h_c , the E values will be closer and closer to 1 when going deeper into the tree. In other words, it becomes easier and easier for a particle to travel into the tree without being captured: a particle having crossed the first generation would be very likely to proceed until the end of the tree.

In contrast, if h is smaller than h_c , the St increases from one bifurcation to the next, and the E values become closer to 0 as a particle enters the more distal regions of the tree. In other terms, such a tree would filter all particles whatever their mass

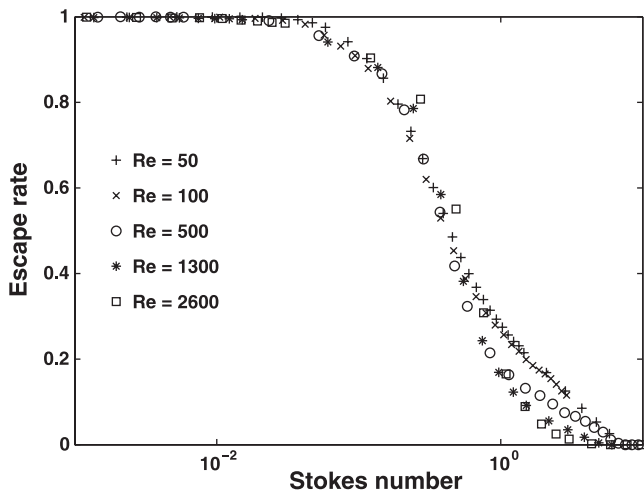


Fig. 6. Escape rate in a single bifurcation as a function of the St of the population of particles for different values of the Re . One can observe a clear collapse onto one unique curve.

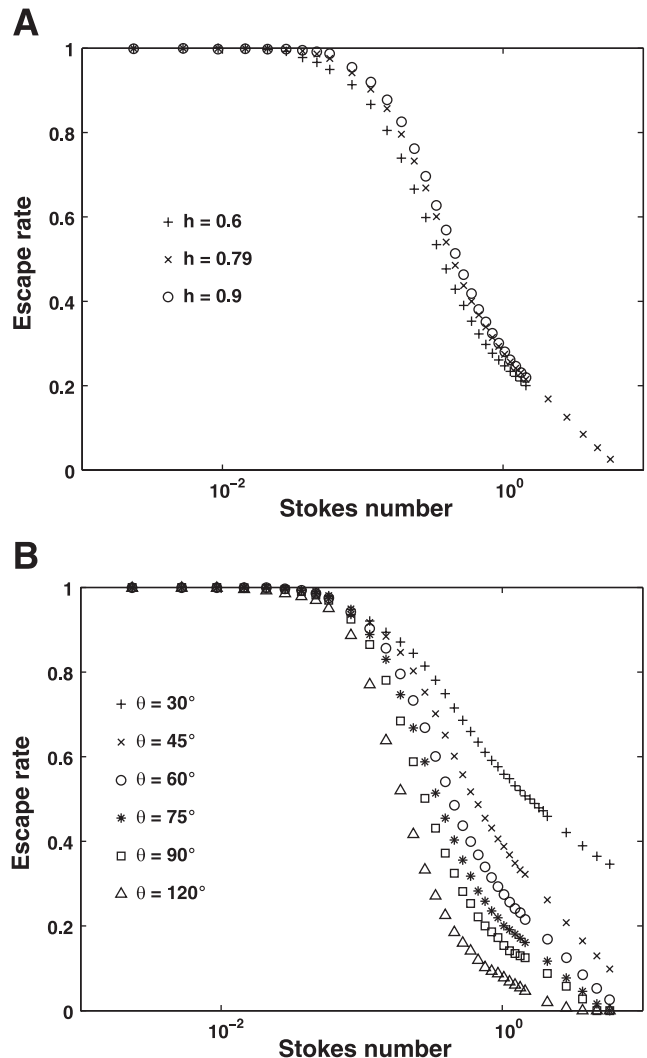


Fig. 7. A: escape rate of single bifurcation for various values of h . B: escape rate of a single bifurcation for various values of θ .

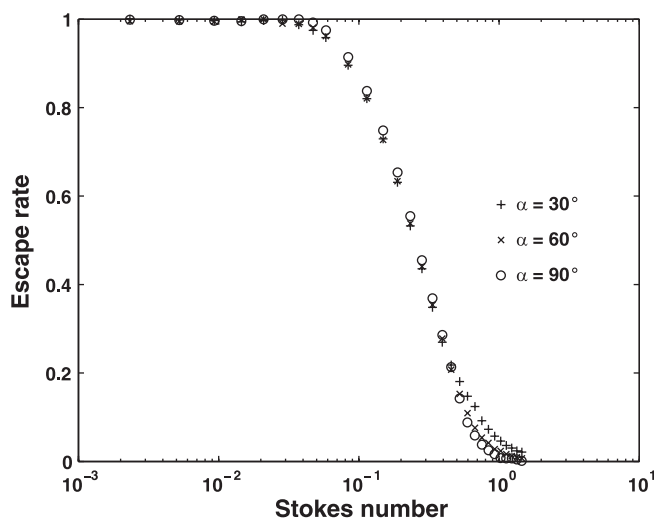


Fig. 8. Robustness of the multiplicative hypothesis: capture rate in a four-generation aerodynamic tree for three different values of α (angle between the planes of two successive bifurcations). The capture rate was almost independent of this angle.

or diameter: the mass and diameter would only determine at which generation the particle is likely to be trapped.

This value h_c thus constitutes a critical threshold that determines the filtering properties of the whole tree. Above h_c , the tree essentially filters the particles in the very first generations; under h_c , all generations of the tree filter smaller and smaller particles so that an infinite tree would theoretically capture all particles. This analysis is of particular interest in the case of the human lung in the low or microgravity environments encountered in astronautical hygiene (8, 10). In Weibel's symmetric model, the human bronchial tree corresponds exactly to the threshold value $h = h_c$ (33, 25). In this light, a population of particles of a given St at the entrance of the trachea would have the same C values at each generation of the tree. Consequently, the number of particles captured would decrease exponentially with the generation with a rate that would only depend on the entrance St .

In fact, precise anatomic measurements of the human bronchial tree (33) have shown that h is not constant among generations. A close examination of the data reveals that the average diameter decreases more rapidly in the first generations (*generations 1–5*) and more slowly in the intermediate bronchial tree (*generations 6–16*). This corresponds to h smaller than h_c in the upper bronchial tree and h larger than h_c in the intermediate tree. In other words, the St of the particles increases at each bifurcation of the upper bronchial tree, which leads to the capture of increasingly smaller particles. In contrast, the St steadily decreases from *generation 6*. This implies that the particles that have reached *generation 6* without being captured are much more likely to proceed deeper and deeper into the bronchial tree, eventually reaching the acinar regions.

Numerical computations using the cascade model described in this report have been carried out for two models of the tracheobronchial tree. The first model is the Weibel's symmetric tree depicted before (with constant scaling), and the second model is a tree whose diameters are determined by actual morphological measurements (33). The C values of a population of particles have been calculated at each bifurcation level

as a function of the particle diameter, assuming a particle density of 2 and an entrance air velocity of 1 m/s, corresponding to a rest condition. The C values of the consecutive bifurcations in Weibel's A model showed that the capture process repeatedly filters the same range of particle sizes, capturing fewer and fewer particles when going deeper into the lung (see Fig. 10A). On the other hand, in the case of the more realistic tree, one can see that h values smaller than h_c of the first generations (*generations 1–4*) lead to an increased filtering of smaller particles (see Fig. 10B). The comparison of both C values (dotted line for the Weibel model and bold line for the more realistic tree in Fig. 10B) showed that this increase of C is particularly significant for particle diameters between 5 and 20 μm . The upper part of the bronchial tree thus appears as the most efficient filtering portion of the entire bronchial tree.

DISCUSSION

At this point, we should make some comments about the results presented in this report. One may question the origin of this multiplicative behavior. To understand how this can happen, one has to recall that the St is the ratio of two quantities, a typical transit time and a relaxation time, which characterizes the duration it takes for a particle to adjust to the flow. Note that particles that are close to the walls have a small velocity and plenty of time to readjust to the flow. In this sense, their capture is small since their "local" St is small. The impacting particles are preferably those that have a large St because they are massive and are at the center of the flow for geometrical reasons. Those particles that escape were initially at the center of the flow and are those that have a short relaxation time, are at the end of a daughter branch, and are more adjusted to the local velocity. In other words, those particles that have escaped are in a situation similar to those that were captured before. This is why the memory of previous captures is lost from a statistical point of view and the capture processes in consecutive bifurcations are independent (32).

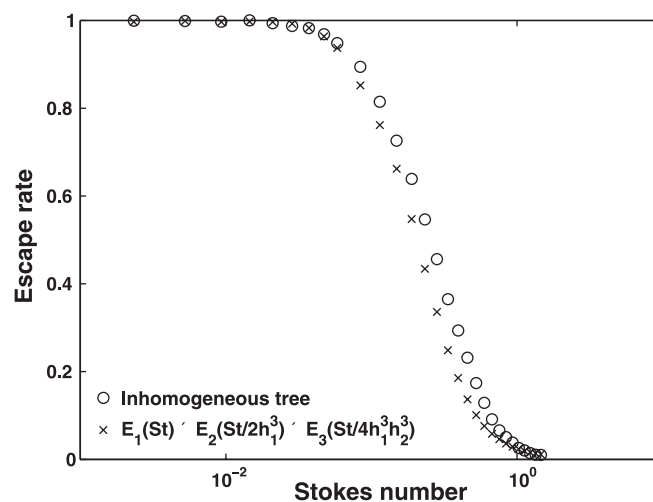


Fig. 9. Escape rates in a tree of varying h values. The h values between *generations 1 and 0* (h_1), *generations 2 and 1* (h_2), and *generation 3 and 2* (h_3) were 0.79, 0.6, and 0.9, respectively. The total escape rate of the whole tree, for any St , was still almost equal to the product of the escape rates of the individual bifurcations corresponding to h_1 , h_2 , and h_3 (E_1 , E_2 , and E_3 , respectively; see Eq. 6).

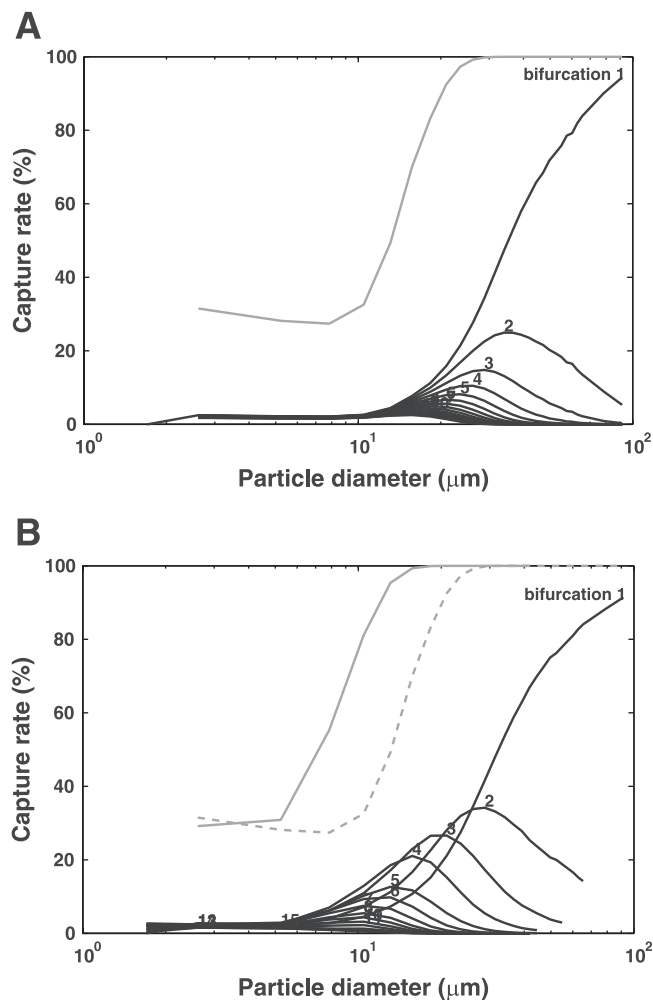


Fig. 10. Capture rates as a function of particle diameter in 2 different tracheobronchial trees of 15 generations computed by the cascade model described in this report. The particle density was taken as equal to 2 and the entrance air velocity in the trachea was 1 m/s (rest condition). *A*: capture rates after each bifurcation for a tree of constant scaling ($h = 2^{-1/3}$), corresponding to Weibel's "A" model. The dotted line represents the total capture rate in the same tree. *B*: capture rates in a tree modeled using morphological measurements of average bronchial diameters (33). The thick line represents the total capture rate in this tree, whereas the dotted line corresponds to Weibel's A model. The first generations (generations 1–5) of the realistic tree capture many more particles of diameters ranging between 5 and 20 μm , thus acting as a "filter" at the entrance of the tracheobronchial tree.

Another important fact is that we can assume flow uniformity in most of the airways. In fact, for Re between 50 and 100, the entrance length divided by the tube diameter (L_e/D) is about $0.03Re$ to $0.06Re$, depending on the desired tolerance (12, 19). Using a value of 0.03, this translates into $L_e < 3D$, which is shorter than the airway. For Re values smaller than 50, L_e/D is ~ 1.5 . Therefore, in a fully developed, parabolic profile, flow is established repetitively at successive generations. Also, the division of the flow in a symmetric branched structure has been shown to be equal for Re values of < 200 (1, 34).

Role of gravity and diffusion. To establish the multiplicative property of the escape process, we have until now considered particles subject only to their inertia and to the drag force exerted by the fluid. Although capture by impaction often represents a very large fraction of the particles trapped into the

lung, this model does not account for the trapping of heavy particles due to sedimentation or the trapping of very small particles in which diffusion plays an essential role. We now examine the respective roles played by gravity and particle diffusion in the capture process.

Gravity modifies the motion of a particle by introducing a constant acceleration term (\vec{g}) in Eq. 3, as follows

$$m \frac{d\vec{u}_p}{dt} = (3\pi\mu d_p)(\vec{u} - \vec{u}_p) + m\vec{g} \quad (7)$$

To compare the respective influences of the drag force and gravity in the impaction process, we computed the typical sedimentation time for a particle falling from the center of a branch of diameter D . Gravity was assumed perpendicular to the axis (O_x) of the branch, which corresponds to the case where its influence is maximal. Along the perpendicular direction (O_y), Eq. 7 becomes:

$$m\dot{y}_p = -(3\pi\mu d_p)\dot{y}_p - mg \quad \text{or} \quad \tau\dot{y}_p = -\dot{y}_p - g\tau$$

$$\text{with } \tau = \frac{m}{3\pi\mu d_p} = \frac{1}{18} \frac{d_p^2 \rho_p}{\mu} \quad (8)$$

Equation 8 reaches constant velocity within milliseconds. Therefore, the motion induced by gravity is essentially a fall at constant velocity $g\tau$ with a typical impaction time (t_1) = $D/(2g\tau)$. Since the typical transit time of any particle along the branch (t_T) = $L/u = 3D/u$, gravity can be neglected for the most part if $t_1 = t_T$. This condition can be expressed in terms of the dimensionless parameters of the problem $Re = uD/\nu$ and $St = \tau u/D$ as follows:

$$t_T = \frac{3D^2}{\nu Re} \ll t_1 = \frac{u}{2gSt}$$

$$= \frac{\nu Re}{2gDSt} \quad \text{or} \quad \frac{Re^2}{6St} \gg \frac{gD^3}{\nu^2} = Ga \quad (9)$$

The righthand side of the last inequality is the Galilei number (Ga), which is proportional to gravity forces divided by viscous forces. The Ga decreases when going down the tree from $Ga = 2.5 \cdot 10^5$ in the trachea to ~ 5 in the last transitional bronchioles (around generation 15). Therefore, viscous forces are predominant to understand impaction when:

$$\frac{6StGa}{Re^2} \ll 1 \quad (10)$$

For a self-similar tree of constant h , the scaling factors of Re , St , and Ga are $1/(2h)$, $1/(2h^3)$, and h^3 , respectively.

Figure 11A shows the values of Re in the canonic tree ($h = 0.79$) for two breathing conditions: rest (flow rate: 250 ml/s) and intense exercise (flow rate: 2,500 ml/s). One can see that the condition of relatively low Re ($Re \leq 200$) is fulfilled distal to generations 3–4 at rest and distal to generation 8 at exercise, respectively. Note that for very quiet breathing (27), smaller flow rates would expand the domain of validity of this condition.

Figure 11B shows a plot of the values of $(6StGa)/Re^2$ against the generation number for two different particle diameters (10 and 30 μm) and the two different breathing flow rates. If we assume of tolerance of 0.3 for this criterion, we are constrained

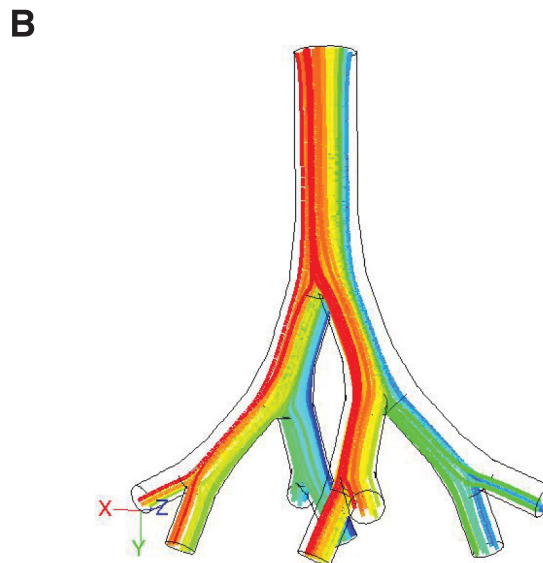
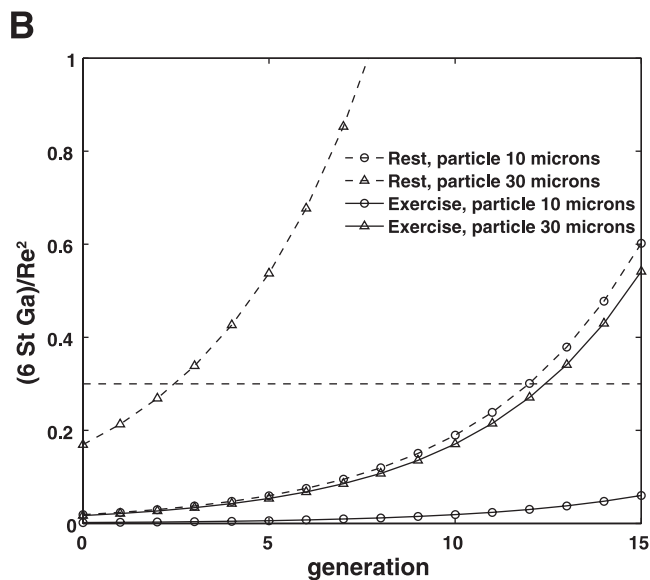
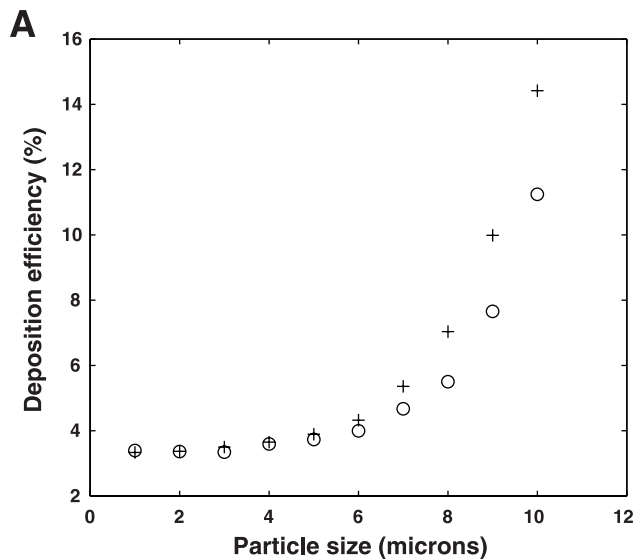
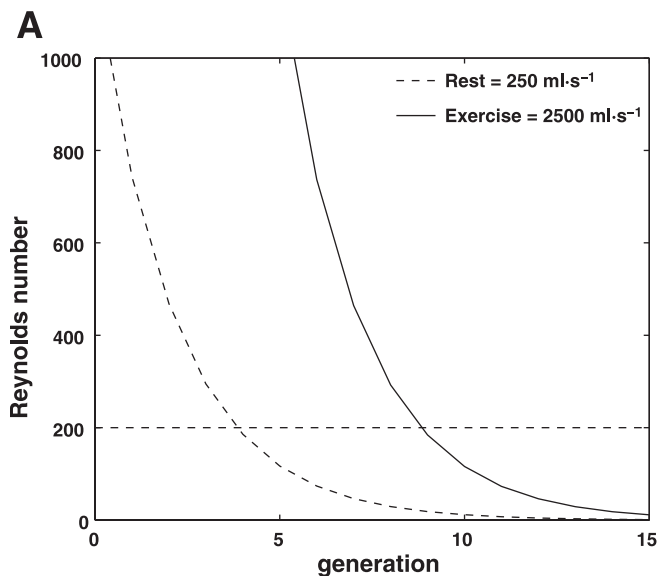


Fig. 11. Influence of gravity effects. *A*: Re in the canonic self-similar tree for two different breathing conditions: at rest (flow rate: 250 ml/s) and at exercise (2,500 ml/s). The horizontal line shows the approximate upper value above which flow uniformity is not satisfied. *B*: ratio between gravity and viscous effects. When this number is larger than 1, gravity effects are predominant in the understanding of the impaction mechanism in the tree. One can see that gravity is predominant only for large particles ($\geq 30 \mu\text{m}$) at rest. The horizontal line shows the upper limit above which one cannot neglect gravity.

to be beyond *generation 3* at rest (flow rate: 250 ml/s), and our assumption is not valid for the 30- μm particle, whereas it is valid up to *generation 12* for the 10- μm particle (Fig. 11). Therefore, our model is accurate for the 10- μm particle for a range of eight to nine generations. At exercise (flow rate: 2,500

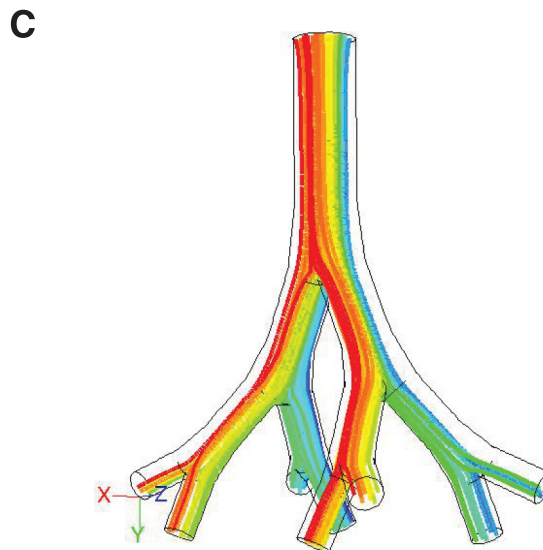


Fig. 12. Influence of gravity effects. *A*: comparison between deposition efficiencies of aerosol particles without or with gravity. Computations were performed on a four-generation tree between *generations 9* and *13*. $Re = 100$. One can see that the deposition efficiencies are very similar up to a size of $\sim 8 \mu\text{m}$. *B*: particle trajectories for 4- μm particles without *C*: particle trajectories for 4- μm particles with gravity.

ml/s), the range of validity of our model is from *generation 8* to *generation 12* for the 30- μm particle and from *generation 8* to the end of the tracheobronchial tree for the 10- μm particle (a minimum range of 8 generations). Therefore, one can observe that the viscous forces are in most cases predominant over gravity except for the largest particle (30 μm diameter) at rest. Moreover, such a particle would have a St value very close to 1 and thus would be already trapped by inertial impaction in the very first generations of the branching tree.

As an example, numerical simulations are presented for a four-generation canonical tree with an entrance diameter of ~ 2 mm. Such a tree corresponds on average to *generation 9–13* in Weibel's model. Deposition efficiencies were computed for particle sizes in the range of 0.1 μm –10 μm , which are the typical aerosol sizes used in systemic delivery. Moreover, much larger particles would be very unlikely to be found at this depth of the tracheobronchial tree. The aerodynamic flow has a Re of 100. Figure 12A shows a comparison of deposition efficiencies without or with gravity. In the second case, the deposition efficiencies were averaged on four different possible directions of gravity. One can observe the very close similarity of both curves up to ~ 8 μm . Figure 12B and 12C show particle trajectories without or with gravity. One cannot observe any noticeable difference. However, gravity certainly plays a role in general in the deposition process, and future studies should investigate how it can be included in the multiplicative behavior observed in the absence of gravity.

The case of diffusion is very different. Diffusion is a stochastic motion that plays a role only for smaller particles (~ 0.1 μm diameter and smaller). Moreover, diffusion is a Markov process that is without memory. Its contribution to deposition is, by essence, independent between successive generations. Therefore, one can add diffusion to our model without breaking its multiplicative property, which is its core property.

Finally, our model does not account for the nonstationary effects that occur, for example, during the flow reversal between inspiration and expiration (4).

The multiplicative model allowed us to predict from first principles the deposition efficiency in the lung in a broad range of generations for various particle sizes and breathing conditions. This can be of practical use especially in the more distal regions of the tracheobronchial tree (*generations 7–17*) when geometrical and anatomic measurements are scarce or only consist of statistical data (11) although modeling of the behavior of very fine particles (smaller than 0.1 μm) still requires the inclusion of diffusion. A systematic, predictive, and probabilistic approach could thus be a useful substitute to computational fluid dynamic approaches in these regions to obtain a first estimate of the deposition efficiency with a minimal computation time. One can, for example, consider hybrid simulations in which the deposition would be computed through computational fluid dynamic simulations in the upper bronchial tree and then provide the data of the population of particles as an input to our probabilistic model.

Finally, this multiplicative model should be seen as a fundamental template of the escape (or capture) process in a tree. It allows us more generally to disentangle in real structures the small contributions due to the details of the

geometry and the specific conditions from the main background process. In that sense, it must not be considered as an alternative to detailed simulations in anatomically based structures but used as a fundamental statistical tool hand in hand with, possibly, patient-based approaches.

Conclusions. The capture of particles transported by advection into an aerodynamic flow in a branched tree structure is usually seen as a very complex problem. Nevertheless, if considered statistically, this phenomenon obeys in first approximation a very simple rule: the capture in each generation is almost independent of the other generations. For a given generation, it is essentially driven by the St of the particles at that generation. In this context, the capture in a tree appears as a cascade process in which the number of particles captured by the structure can then be directly estimated by simply multiplying the E values of each generation. These E values directly depend on the local St of the particles at each generation, which, for a tree, can in turn be expressed in terms of the St at the tree entrance and of the h values of the geometry from one generation to the next. Applying these results to simplified models of the human lung, we predict that particles are either deposited in the upper bronchial tree or reach the deepest acinar regions of the respiratory system. More generally, our results indicate that particle deposition in the entire intermediate bronchial tree can be understood through the successive computation of trapping in successive bifurcations, each being done in a realistic detailed geometry, a feasible goal.

GRANTS

This work was supported by the Brazilian agencies Coordenação de Aperfeiçoamento de Pessoal de Nível Superior, Conselho Nacional de Desenvolvimento Científico e Tecnológico, Fundação Cearense de Apoio ao Desenvolvimento Científico e Tecnológico, and Financiadora de Estudos e Projetos and by the French agency Comité Français d'Évaluation de la Coopération Universitaire et Scientifique avec le Brésil. Financial support was also provided by the Ecole Polytechnique and Agence Nationale de la Recherche Project ANR 05-SEST-001.

DISCLOSURES

No conflicts of interest, financial or otherwise, are declared by the author(s).

REFERENCES

1. Andrade JS, Alencar AM, Almeida MP, Filho JM, Buldyrev SV, Zapperi S, Stanley HE, Suki B. Asymmetric flow in symmetric branched structures. *Phys Rev Lett* 81: 926–929, 1998.
2. Apiou-Sbirlea G, Katz IM, Martonen TB. The effects of simulated airway diseases and affected flow distributions on aerosol deposition. *Resp Care* 55: 707–718, 2010.
3. Ashgarian B, Price OT, Hofmann W. Prediction of particle deposition in the human lung using realistic models of lung ventilation. *J Aerosol Sci* 37: 1209–1221, 2006.
4. Butler JP, Tsuda A. Logistic trajectory maps and aerosol mixing due to asynchronous flow at airway bifurcations. *Resp Physiol Neurobiol* 148: 195–206, 2005.
5. Comer JK, Kleinstreuer C, Kim CS. Flow structures and particle deposition patterns in double bifurcation airway models. Part 2. Aerosol transport and deposition. *J Fluid Mech* 435: 55–80, 2001.
6. Comer JK, Kleinstreuer C, Zhang Z. Flow structures and particle deposition patterns in double bifurcation airway models. Part 1. Air flow fields. *J Fluid Mech* 435: 25–54, 2001.
7. Darquenne C, Paiva M, West JB, Prisk GK. Effect of microgravity, and hypergravity on deposition of 0.5- to 3- μm -diameter aerosol in the human lung. *J Appl Physiol* 83: 2029–2036, 1997.
8. Darquenne C, Prisk GK. Deposition of inhaled particles in the human lung is more peripheral in lunar than in normal gravity. *Eur J Appl Physiol* 103: 687–695, 2008.

9. **Darquenne C, West JB, Prisk GK.** Deposition, and dispersion of 1- μm aerosol boluses in the human lung: effect of micro- and hypergravity. *J Appl Physiol* 85: 1252–1259, 1998.
10. **Darquenne C, West JB, Prisk GK.** Dispersion of 0.5- to 2- μm aerosol in μG and hypergravity as a probe of convective inhomogeneity in the lung. *J Appl Physiol* 86: 1402–1409, 1999.
11. **Florens M, Sapoval B, Filoche M.** An anatomical and functional model of the human tracheobronchial tree. *J Appl Physiol* 110: 756–763, 2011.
12. **Golberg IS, Folk RT.** Solutions for steady and nonsteady entrance flow in a semi-infinite circular tube at very low Reynolds-numbers. *Siam J Appl Math* 48: 770–791, 1988.
13. **Heyder J, Gebhart J, Rudolf G, Schiller CF, Stahlhofen W.** Deposition of particles in the human respiratory tract in the size range 0.005–15 μm . *J Aerosol Sci* 17: 811–825, 1986.
14. **Hinds WC.** *Aerosol Technology: Properties, Behavior, and Measurement of Airborne Particles*. New York: Wiley, 1999.
15. **Hofmann W, Balashazy I, Heistracher T.** The relationship between secondary flows and particle deposition patterns in airway bifurcations. *Aerosol Sci Technol* 35: 958–968, 2001.
16. **Isaacs KK, Schlesinger RB, Martonen TB.** Three-dimensional computational fluid dynamics simulations of particle deposition in the tracheobronchial tree. *J Aerosol Med* 19: 344–352, 2006.
17. **Isabey D.** Steady and pulsatile flow distribution in a multiple branching network with physiological applications. *J Biomech* 15: 395–404, 1982.
18. **Johnston JR, Isles KD, Muir DCF.** Inertial deposition of particles in human branching airways. In: *Inhaled Particles IV*, edited by Walton WH. Oxford: Pergamon, 1977, p. 61–72.
19. **Lew HS, Fung YC.** Entry flow into blood vessels at arbitrary Reynolds number. *J Biomech* 3: 23–38, 1970.
20. **Li Z, Kleinstreuer C, Zhang Z.** Particle deposition in the human tracheobronchial airways due to transient inspiratory flow patterns. *J Aerosol Sci* 38: 625–644, 2007.
21. **Luo HY, Liu Y, Yang XL.** Particle deposition in obstructed airways. *J Biomech* 40: 3096–3104, 2007.
22. **Martin AR, Finlay WH.** A general algebraic equation for predicting total respiratory tract deposition of micrometer-sized aerosol particles in humans. *J Aerosol Sci* 38: 246–253, 2006.
23. **Martonen TB, Schroeter JD, Hwang DM, Fleming JS, Conway JH.** Human lung morphology models for particle deposition studies. *Inhal Toxicol* 12: 109–121, 2000.
24. **Martonen TB, Zhang Z, Yu G, Musante CJ.** Three-dimensional computer modeling of the human upper respiratory tract. *Cell Biochem Biophys* 35: 255–261, 2001.
25. **Mauroy B, Filoche M, Andrade JS, Sapoval B.** Interplay between geometry and flow distribution in an airway tree. *Phys Rev Lett* 90: 148101, 2003.
26. **Mauroy B, Weibel ER, Filoche M, Sapoval B.** An optimal bronchial tree may be dangerous. *Nature* 427: 633–636, 2004.
27. **Nodelman V, Ultman JS.** Longitudinal distribution of chlorine absorption in human airways: a comparison to ozone absorption. *J Appl Physiol* 87: 2073–2080, 1999.
28. **Nowak N, Kakade PP, Annapragada AV.** Computational fluid dynamics simulation of airflow and aerosol deposition in human lungs. *Ann Biomed Eng* 31: 374–390, 2003.
29. **Schlesinger RB, Bohning DE, Chan TL, Lippman M.** Particle deposition in a hollow cast of the human tracheobronchial tree. *J Aerosol Sci* 8: 445–449, 1977.
30. **Snyder B, Dantzker DR, Jaeger MJ.** Flow partitioning in symmetric cascades of branches. *J Appl Physiol* 51: 598–606, 1981.
31. **Van Erbruggen C, Hirsch C, Paiva M.** Anatomically based three-dimensional model of airways to simulate flow and particle transport using computational fluid dynamics. *J Appl Physiol* 98: 970–980, 2005.
32. **Vasconcelos TF.** *Transport de Particules dans des Structures Irregulieres* (PhD thesis). Palaiseau, France: Ecole Polytechnique, 2007.
33. **Weibel ER.** *Morphometry of the Human Lung*. New York: Springer Verlag and Academic, 1963.
34. **Wilquem F, Degrez G.** Numerical modeling of steady inspiratory airflow through a three-generation model of the human central airways. *J Biomech Eng* 119: 59–65, 1997.
35. **Zhang ZE, Kleinstreuer C.** Effect of particle inlet distributions on deposition in a triple bifurcation lung airway model. *J Aerosol Med* 14: 1 and 13–29, 2001.